URSI AP-RASC 2019, New Delhi, India, 09 - 15 March 2019

Computer simulations of 434 MHz Electromagnetic Phased Array for thermal therapy of locally advanced breast cancer

Divya Baskaran, Kavitha Arunachalam*
Department of Engineering Design, Indian Institute of Technology Madras, Chennai 600036, India.

Abstract

A phased array applicator is proposed for the treatment of locally advanced breast cancer using a 434 MHz cavity backed patch antenna as the array element. 3D coupled multi-physics modeling is used to convert the power deposited by the phased array applicator to temperature distribution. The performance of the proposed applicator is evaluated using an anatomically realistic 3D breast model of a patient with locally advanced tumour (35043 mm^3). The focusing ability of the phased array is demonstrated using heterogeneous tissue specific dispersive dielectric model. 3D electromagnetic (EM) simulations indicate 25% iso-SAR coverage in more than 75 % of the tumor volume. Thermal simulations indicate selective elevation of tumour temperature to the hyperthermia temperature range with very limited hot spots in the healthy tissues.

Keywords: breast cancer, hyperthermia treatment, patch antenna, phased array, thermal therapy.

1. Introduction

Hyperthermia treatment (HT) is the elevation of the tissue or whole body temperature to 41 °C – 45 °C for duration of 30-60 minutes. Heat increases the blood flow to the cancer cells which renders them more sensitive to high energy radiation and drugs. Thus, addition of HT to radiotherapy (RT) and chemotherapy (CT) treatment of cancer has been demonstrated as an effective adjuvant therapy. The population based cancer registry indicates that breast cancer is the most frequent cancer among the women in India and it accounts for 25% of all female malignancies with 1.67 million new cancer cases in 2012 [1]. Almost 54 % of the breast cancer are diagnosed at the advanced stage of cancer, where the tumor size would reached up to 4 to 5 cm. The major treatment options for breast cancer namely surgery, RT and CT do not always eliminate all viable cancer cells especially in the case of advanced tumors, which may lead to the recurrence. The use of thermal therapy as an adjuvant to RT/CT in the pre or post-operative condition have been demonstrated to significantly improve the complete response (CR), especially for breast cancer and chest wall recurrence of breast cancer. A randomized clinical trial on 120 patients with breast cancer demonstrated an increase in CR rate from 23.5 % to 68.2 % in RT alone and RT + HT cases respectively [2].

Loco-regional deep hyperthermia treatment can be accomplished using phased array of antennas. The amplitude and phase excitation of each antenna in the phased array applicator can be varied to move the focus point within the patient body. Investigation of the phased array applicator for HT of breast cancer began with the development of dual channel adaptive microwave phased array using 915 MHz waveguides [3]. The bulky waveguide applicator was then replaced by a 140 MHz RF phased array [4], 915 MHz tapered microstrip patch [5], and 915 MHz patch antennas with conformal ground plane [6]. These phased array applicators either lack power steering ability and hotspot control or incapable to treat large locally advanced tumors. In this paper we present a phased array applicator designed using 434 MHz cavity backed antenna array for hyperthermia treatment of locally advanced breast cancer. The ability of the phased array applicator to selectively elevate tumour tissue temperature with minimal hot spots in the healthy tissues is demonstrated using coupled electromagnetic and thermal simulations for an anatomically realistic 3D model of a patient breast with locally advanced breast tumour.

2. Materials and Methods

2.1 434 MHz applicator phased array

The cavity backed c-type patch antenna proposed in [7] was selected as the basic element for phased array design. The metal cavity surrounding the radiating patch lowered the mutual coupling between antennas in the array configuration. The antennas were arranged in multi-ring cylindrical configuration surrounding the breast which has been proved to possess excellent steering ability. The proposed phased array applicator was constructed with 18 antennas arranged in 3 rings with 6 antennas per ring on the inner surface of an open polygonal tank filled with de-ionized water. The 18 element phased array applicator provided adequate degree of freedom for axial and lateral steering of the radiated EM field inside the breast suspended in the water filled tank. The antennas were placed at $\lambda_{water}/2$ distance away from the breast tissue to avoid self-resonance inside the tank and influence of the

tissue loads with the antenna performance. Antenna rings were interspaced for enhanced target coverage and to reduce mutual coupling between antennas.

2.2 3D breast model

Anatomically realistic 3D heterogeneous breast model of a patient image data from the cancer imaging archive (TCIA) [8] was used to investigate the spatial temperature control of the proposed 434 MHz phase array applicator. MR breast image of a patient with locally advanced cancer (size > 4 cm) was chosen for the simulation. The images were contrast enhanced and segmented into adipose tissue, fibro glandular region, cancer, skin and chest wall based on the intensity levels. Segmented regions were smoothened and holes, islands were removed using morphological operator. Each 2D segmented region was volume rendered to 3D by marching cube algorithm. Figure 1 shows the heterogeneous 3D model of a patient breast segmented into different breast tissues. Each tissue type was subdivided into tetrahedral mesh and the mesh density determined to trade-off between simulation accuracy and computational time.

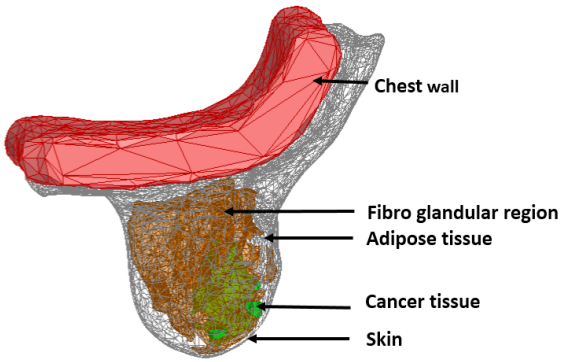

Figure 1. 3D segmented breast model of a patient MR data from TCIA.

2.3 Electromagnetic simulation

EM simulations were carried out in 3D finite element based solver (HFSS ®, Ansys Inc., USA). The antennas in the array configuration exhibited return loss ($-20\log_{10}|S_{ii}|$) greater than 15 dB and coupling loss ($-20\log_{10}|S_{ij}|$)) more than 30 dB where S_{ij} is the scattering parameter calculated between the input ports of the i^{th} and j^{th} antennas. The segmented 3D breast model was immersed inside the deionized water tank with the chest wall lying outside the tank as shown in Figure 2. This position is similar to patient lying on the bed with the breast in pendent position. The dielectric property of the individual breast tissue was assigned using the Cole-Cole models reported by Gabriel et al [9]. The water tank was suspended inside an air box. The input ports of the antennas were excited with wave port. The air box was terminated with radiation boundary condition. Simulation was carried out for continuous wave excitation at 434 MHz.

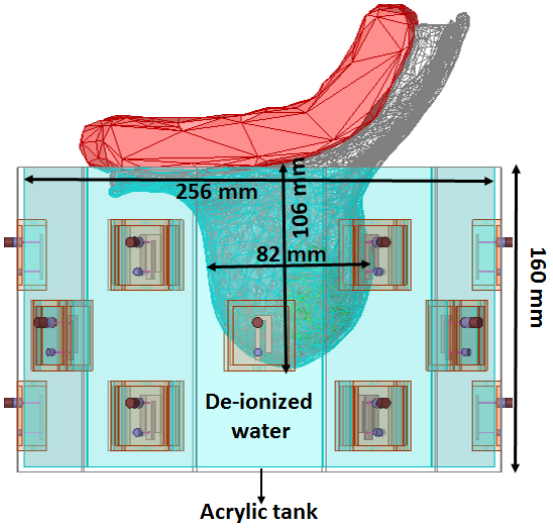

Figure 2. 3D EM model of the phased array applicator with the 3D heterogeneous breast model suspended in the water filled tank.

2.4 Hyperthermia treatment planning

The phase and amplitude of the excitation of each antenna to steer the radiated EM fields to the tumour tissue was determined using reciprocity theorem. A virtual point source was placed in the target location where maximum power deposition is anticipated. The wavefront from a virtual point source at the target location was allowed to propagate to each antenna through the heterogeneous breast model and was captured at the excitation port of each antenna. The conjugate of the induced phasor field at each antenna port was used as the antenna's input excitation. The relative change in the induced field strength and phase delay calculated with respect to a reference antenna was used to excite the phased array applicator to focus the radiated EM fields in the tumour tissue. The power radiated by each antenna was limited to 5 W in the numerical simulation.

2. 5 Thermal simulation

Thermal simulations were carried out in COMSOL Multiphysics® to study the temperature rise in the 3D heterogeneous breast model induced by the antenna array. The individual breast tissue was assigned thermal properties according to [10]. Convective boundary condition was assigned on the skin surface in contact with the deionized water. The heat transfer coefficient was set as 100 W/ m^2 K for the skin surface which mimicked the circulation of temperature controlled de-ionized water during hyperthermia treatment. Initially, all tissue regions were maintained at 37 ºC before the treatment procedure was initiated. The water inside the tank was maintained at 22 ºC throughout the treatment procedure. The power distribution in each tissue region calculated in HFSS was assigned as the heat source in the thermal simulation. The

temperature distribution inside the breast was obtained by solving Penne's bio heat transfer equation [10],

$$\rho C\frac{\partial T(\vec{r},t)}{\partial t}+\nabla.(-k\nabla T(\vec{r},t)-\omega_b\rho_b c_b(T_a-T(\vec{r},t)) +Q_m+P(\vec{r},t) \quad =0 \qquad (1).$$

In Eqn. (1), ρ , C are the density and specific heat capacity of tissue, $T(\vec{r},t)$ is the temperature distribution at position $\vec{r}$ at time t, k is the thermal conductivity, ω_b,ρ_b and c_b are the perfusion rate, density and specific heat capacity of blood respectively, Q_m is the tissue metabolic rate and $P(\vec{r},t)$ is the power distribution. Time dependent simulations were carried out with the sources ON for initial 30 minutes and OFF for the rest of the time. The temperature monitoring probes are placed in all tissue regions to record the temperature rise over the period of time.

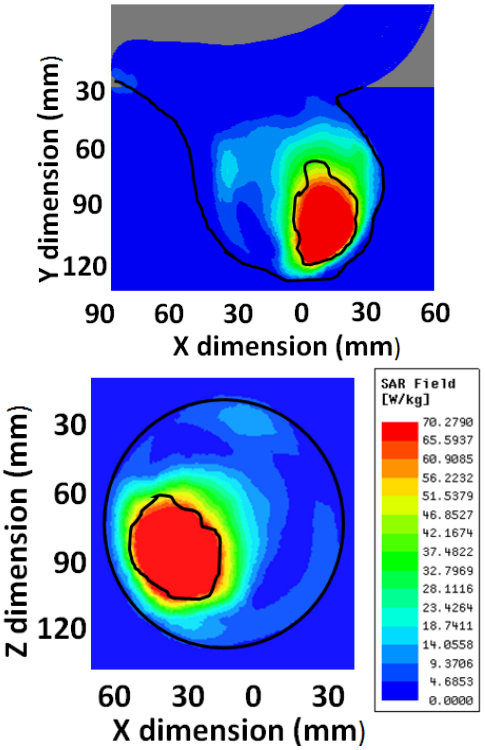

Figure 3. Tissue SAR distribution in the XY and XZ planes through the tumour tissue at 434 MHz.

3. Results and discussion

Figure 3 shows the simulated specific absorption rate (SAR) of the tissue in the transverse mid planes of the tumour. Figure 3 shows that the maximum SAR deposited inside the tumour compared to the surrounding healthy tissues. In Figure 3, the boundaries of the tumor and adipose tissues are indicated by black line. The simulation result suggests good focusing ability in a realistic breast model using the proposed array configuration and treatment planning algorithm. The histogram of the SAR deposited in the individual tissues is shown in Figure 4. It is evident in Figure 4 that SAR value in the tumor tissue is higher than the SAR values in the adipose, glandular, skin and chest wall tissues. Also, more than 75 % of the tumor volume is covered by 25 % of maximum SAR (25 % iso-SAR) in the tumour tissue. Figure 5 shows the temperature rise in each tissue regions calculated for the ON and OFF period of the phased array excitation. It is evident in Fig. 5 that the tissue temperature rises very sharply in the tumour region compared to the other tissue regions. The temperature rises sharply during initial 600 s of the heating procedure and then it gradually attains the thermal equilibrium with the blood perfusing in the tissue. The tissue temperature fell sharply when the phased array excitation sources were switched OFF. The thermal simulation results are in good agreement with the simulated SAR. The reduced skin temperature seen in Figure 4 is due to the convective cooling effect of the circulating temperature controlled de-ionized water bolus.

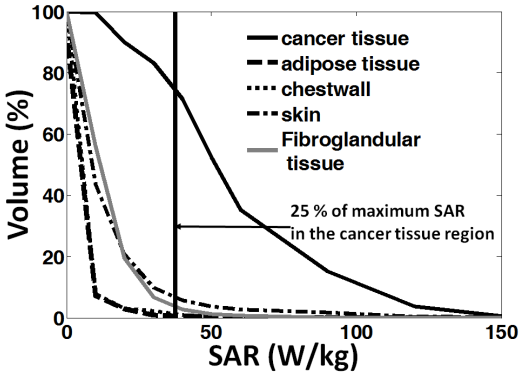

Figure 4. SAR – volume histogram of each tissue region

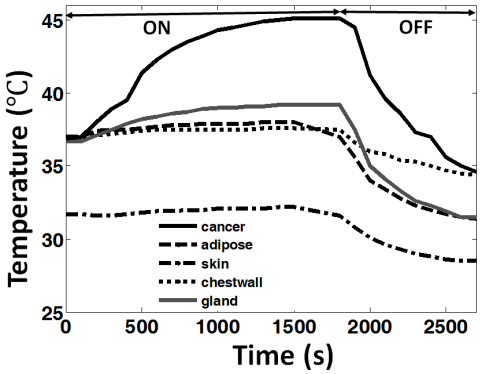

Figure 5. Temperature against time in recorded each tissue region

The coupled EM and thermal simulation results for an anatomically realistic 3D breast model demonstrate the ability of the proposed 434 MHz phase array applicator to focus selectively in the large tumour target with acceptably low hot spot in the healthy tissue for HT of locally advanced breast cancer.

4. Conclusion

In this work we presented the feasibility study of hyperthermia treatment of locally advanced breast cancer using the proposed 434 MHz phased array applicator. The focusing ability of phased array applicator at 434 MHz was evaluated using an anatomically realistic 3D breast model. Both electromagnetic and thermal simulations demonstrated that the phased array applicator can selectively heat the tumour tissue with limited hotspots in the surrounding healthy tissues. The steering ability of the phased array will be verified using diverse patient data prior to applicator fabrication and experimental verification in tissue mimicking phantoms.

5. References

1. Nounou, M.I., F. ElAmrawy, N. Ahmed, K. Abdelraouf, S. Goda, and H. Syed-Sha-Qhattal, "Breast Cancer: Conventional Diagnosis and Treatment Modalities and Recent Patents and Technologies," *Breast Cancer (Auckl)*, **9**, Suppl 2, 2015, pp. 17-34, doi: 10.4137/bcbcr.s29420.

2. Jones, E.L., J.R. Oleson, L.R. Prosnitz, T.V. Samulski, Z. Vujaskovic, D. Yu, L.L. Sanders, and M.W. Dewhirst, "Randomized trial of hyperthermia and radiation for superficial tumors," *J Clin Oncol*, **23**, 13, May 1 2005, pp. 3079-85, doi: 10.1200/jco.2005.05.520.

3. Gardner, R.A., H.I. Vargas, J.B. Block, C.L. Vogel, A.J. Fenn, G.V. Kuehl, and M. Doval, "Focused microwave phased array thermotherapy for primary breast cancer," *Ann Surg Oncol*, **9**, 4, May 2002, pp. 326-32.

4. Wu, L., R.J. McGough, O.A. Arabe, and T.V. Samulski, "An RF phased array applicator designed for hyperthermia breast cancer treatments," *Physics in medicine and biology*, **51**, 1, 12/15 2006, pp. 1-20, doi: 10.1088/0031-9155/51/1/001.

5. Stang, J., M. Haynes, P. Carson, and M. Moghaddam, "A preclinical system prototype for focused microwave thermal therapy of the breast," *IEEE Trans Biomed Eng*, **59**, 9, Sep 2012, pp. 2431-8, doi: 10.1109/tbme.2012.2199492.

6. Curto, S., A. Garcia-Miquel, M. Suh, N. Vidal, J.M. Lopez-Villegas, and P. Prakash, "Design and characterisation of a phased antenna array for intact breast hyperthermia," *Int J Hyperthermia*, **34**, 3, May 2018, pp. 250-260, doi: 10.1080/02656736.2017.1337935.

7. Chakaravarthi, G. and K. Arunachalam, "Design and characterisation of miniaturised cavity-backed patch antenna for microwave hyperthermia," *Int J Hyperthermia*, **31**, 7, 2015, pp. 737-48, doi: 10.3109/02656736.2015.1068957.

8. Clark, K., B. Vendt, K. Smith, J. Freymann, J. Kirby, P. Koppel, S. Moore, S. Phillips, D. Maffitt, M. Pringle, L. Tarbox, and F. Prior, "The Cancer Imaging Archive (TCIA): Maintaining and Operating a Public Information Repository," *Journal of Digital Imaging*, **26**, 6, 2013/12/01 2013, pp. 1045-1057, doi: 10.1007/s10278-013-9622-7.

9. Gabriel, S., R.W. Lau, and C. Gabriel, "The dielectric properties of biological tissues: II. Measurements in the frequency range 10 Hz to 20 GHz," *Physics in Medicine & Biology*, **41**, 11, 1996, pp. 2251, doi: 10.1088/00319155/41/11/002.

10. Arunachalam, K., P.F. Maccarini, O.I. Craciunescu, J.L. Schlorff, and P.R. Stauffer, "Thermal characteristics of thermobrachytherapy surface applicators for treating chest wall recurrence," *Phys Med Biol*, **55**, 7, Apr 7 2010, pp. 1949-69, doi: 10.1088/0031-9155/55/7/011.